Piezoelectric tuning fork biosensors for the quantitative measurement of biomolecular interactions

2015 Nanotechnology 26 495502

(http://iopscience.iop.org/0957-4484/26/49/495502)

IOP Publishing Nanotechnology
Nanotechnology 26 (2015) 495502 (9pp) doi:10.1088/0957-4484/26/49/495502

Piezoelectric tuning fork biosensors for the quantitative measurement of biomolecular interactions

Laura Gonzalez[1,3], Mafalda Rodrigues[2], Angel Maria Benito[1], Lluïsa Pérez-García[2], Manel Puig-Vidal[1] and Jorge Otero[1]

[1] SIC-BIO, Bioelectronics and Nanobioengineering Group, Department of Electronics, University of Barcelona, C/Marti i Franques, 1, E-08028 Barcelona, Spain
[2] Department of Pharmacology and Therapeutic Chemistry, University de Barcelona, Av. Joan XXIII s/n, E-08028 Barcelona, Spain

E-mail: manuel.puig@ub.edu

Received 18 June 2015, revised 22 September 2015
Accepted for publication 22 October 2015
Published 17 November 2015

Abstract

The quantitative measurement of biomolecular interactions is of great interest in molecular biology. Atomic force microscopy (AFM) has proved its capacity to act as a biosensor and determine the affinity between biomolecules of interest. Nevertheless, the detection scheme presents certain limitations when it comes to developing a compact biosensor. Recently, piezoelectric quartz tuning forks (QTFs) have been used as laser-free detection sensors for AFM. However, only a few studies along these lines have considered soft biological samples, and even fewer constitute quantified molecular recognition experiments. Here, we demonstrate the capacity of QTF probes to perform specific interaction measurements between biotin–streptavidin complexes in buffer solution. We propose in this paper a variant of dynamic force spectroscopy based on representing adhesion energies E (aJ) against pulling rates v (nm s^{-1}). Our results are compared with conventional AFM measurements and show the great potential of these sensors in molecular interaction studies.

Keywords: atomic force microscopy, quartz tuning fork, force spectroscopy, protein–protein interactions

(Some figures may appear in colour only in the online journal)

1. Introduction

The quantitative measurement of the interactions between biomolecules is currently a hot topic in molecular biology research [1–4]. About 60% of all pharmaceuticals have membrane proteins as their main target [5–7], so measurement of protein–protein interactions is of special interest; results can provide crucial insight into how receptors in the cell membrane react to different molecules. Several techniques are being successfully used to measure protein–protein interactions (see [8, 9] for further details); among them, atomic force microscopy (AFM) is of special interest because it can be employed to obtain high-resolution molecular images and to measure the unbinding force of individual ligand–receptor complexes directly [10]. For instance, glucagon/anti-glucagon pairs are studied in [11] under different pH values and it is shown that the pH dependence of antigen–antibody bond forces can be measured with an AFM sensor. In [12], the spatial organization of the peptidoglycan on the cell walls of living bacteria is studied and in [13] antigen–antibody binding forces in lymphoma patient cancer cells are measured to find potential effective targets for cancer drugs. AFM functions through measuring the interaction forces between a nanometric tip, placed at the end of a micro-fabricated cantilever, and the sample surface. The forces are

[3] Current address: Universidad Regional Amazónica IKIAM, Tena, Ecuador.

detected by means of the reflection of a laser beam from the rear side of the cantilever which is measured using a position-sensitive photodiode. Beyond its use as an imaging tool, AFM can also measure the interaction forces between the tip and the sample: the so-called force spectroscopy mode. The streptavidin–biotin system was one of the first to be studied at the single molecule level using force spectroscopy, due to its high affinity and specificity of interaction [14–16]. The basics of these measurements is certainly straightforward: one of the biomolecules is linked on the tip, the other one is immobilized on the surface, and the interaction force versus the tip-sample distance is recorded in a series of experiments. After data analysis, some parameters of the interaction can be quantified. The dissociation rate k_0 can be determined after a dynamic study over different pulling speeds between the ligand–receptor pair and parameters related to the binding potential can be obtained which are related to the energy landscape of the bond studied [17, 18].

One of the main applications of the measurement of protein interactions is molecular recognition: AFM is used as a biosensor to determine the degree of affinity between biomolecules [19, 20]. In recent years, efforts have been made to incorporate the AFM force detection scheme into compact biosensors. The reported solutions have focused on developing chips that are compatible with the optical readout [21, 22] or on the integration of laser-free sensors, mainly cantilevers with piezoresistive readout [23]. Nevertheless, the development of these cantilever-based biosensors requires specific micro-fabrication facilities, usually involving non-standard fabrication steps, which is a huge drawback for progress in this research field and limits it to a few research groups around the world [24, 25]. However, the use of nanosensors based on a quartz tuning fork (QTF) is a promising alternative to the conventional silicon cantilevers [26–29] and it has been widely used for sample imaging and nanocharacterization [30–32]. Instead of the optical detection system used in conventional AFM, the mechanical oscillation of the QTF is transduced into a piezoelectric current and detected by a transimpedance amplifier (TIA). Moreover, tuning forks show additional advantages such as low stable amplitude A, a high quality factor Q and a high spring constant K, which permit detection of forces in the pico-range [33]. Also, QTFs do not present one of the main problems of cantilevers: thermal drift (due to the heat dissipation of the laser diode or due to the intrinsic properties of piezoresistive materials). To build QTF-based sensors, a sharpened tip is attached to one of the prongs of a piezoelectric resonator and oscillated, parallel to the sample surface in shear force mode [34]; or perpendicular to the surface in perpendicular mode [35]. When a force acts on the tip, there is a change in the resonant frequency of the sensors (which can be measured as a change in the vibration amplitude if working at a constant excitation frequency) [36].

QTF-based nanosensors have been used to image cells [30], bacteria [37] and biomolecules [38]. Sub-molecular resolution in air has also been obtained in [39] and qualitative recognition has been performed between avidin and lysozyme antibody in [40] in shear mode. Nevertheless, there are few studies of quantitative molecular interaction forces with such a probe in solution. In [41], bovine serum albumin protein stretching is studied using three different chemically-terminated tips in aqueous media with the QTF sensors quantifying the withdrawal forces. This employs the piezoelectric resonator oscillating perpendicular to the sample surface using amplitude modulation (AM-AFM) control. Small non-linear jumps in the phase curve are observed when an unbinding event occurs between ligand and receptor. After a series of assumptions, the phase variations are translated into a force gradient curve, but the measurements are not quantified in energy terms, so they cannot be compared with results obtained using alternative methods.

Here, we present the application of QTF probes for molecular interaction analysis between biotin–streptavidin complexes. We apply a variant of the dynamic force spectroscopy (DFS) technique commonly used for AFM systems to QTF working in shear force detection. DFS consists of measurements of the force needed to unbind individual receptor–ligand systems. Nevertheless, we measure the adhesion energies of the biotin–streptavidin system at different pulling velocities and compare our results to those obtained from AFM measurements under the same experimental conditions. Adhesion energy [42, 43] is the parameter that it is possible to measure directly from the amplitude–distance curves obtained with QTF sensors. In this work, we demonstrate the effectiveness of piezoelectric QTF sensors in shear mode to perform specific interaction measurements between a ligand and its receptor in liquid media.

2. Materials and methods

2.1. Sensor production and operation

In our experiments we used QTFs with a resonance frequency of 32 768 Hz (model *AB*38*T*, Abracon Corp., USA). The nanosensors were custom made by attaching the functionalized probe to one of the prongs of a decapsulated QTF. The quality factor (Q) of these QTFs is as high as 100 000 when packaged in vacuum. The device is then decapsulated and the probe is glued to one tine of the fork. The Q factor falls because the quartz structure is resonating in air instead of vacuum and due to the added mass of the fiber. A probe length of 3–4 mm is enough to work with the fiber tip inside a liquid cell but with the fork resonating in the air.

As a prior step to functionalization, the optical fiber (SiO_2) was chemically sharpened [44]. In brief, a 125 μm optical fiber was immersed in a 40% HF solution, with an organic solvent (iso-octane C_8H_{18}) on top to protect against the acid vapors; then, a meniscus is formed creating a reaction gradient at the interface between the acid and the solvent, resulting in a self-terminating process after some 90 min. After this etching, the fibers are rinsed with ethanol and water, functionalized with biotin and mounted onto the resonator with cyanoacrylate glue (see figure 1(A)).

The sensor was mounted on an adapted scanning tunneling microscopy head integrated into a commercial AFM microscope (Nanotec Electrónica, Spain). A fully custom-

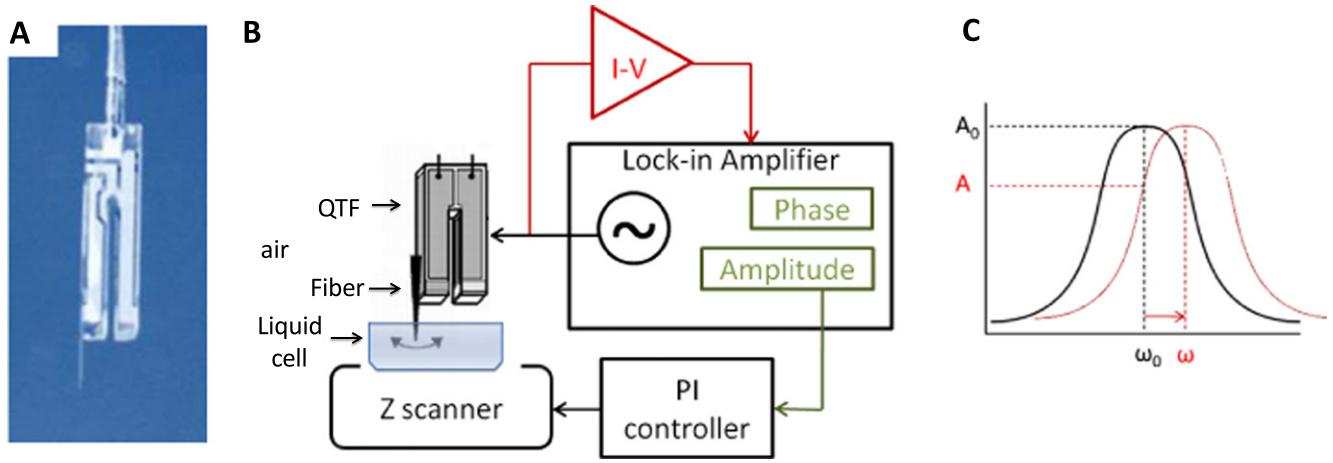

Figure 1. (A) Decapsulated QTF sensor with a fiber probe attached to one of the prongs. (B) Scheme of the QTF measurement setup. The QTF probe is excited electrically with an ac signal by setting the resonance frequency. The current through the device is measured by a lock-in amplifier. (C) Principle of operation in amplitude mode.

made electronic module was used to drive the nanosensor electrically [45] to its resonance frequency. A TIA (model OPA656, Texas Instruments, USA) then converts the current flowing through the QTF into a voltage with a 10^6 V A^{-1} gain. The QTFs were operated in shear mode and in amplitude modulation: oscillating parallel to the sample surface at constant excitation frequency and reading the amplitude and phase variations when an interaction between the tip and the sample is produced (see figure 1(B)). When there is a tip–sample interaction force, the frequency response is shifted and a lower amplitude than the free oscillation amplitude is measured (see figure 1(C)).

For the experiments presented in this work, a QTF with a quality factor, Q, of 1500 and resonance frequency, f, of 34 830 Hz was used (once the fiber was attached and immersed in the buffer solution). A driving amplitude of 20 mV was selected and the current measured at resonance was 5.2 nA, which corresponds to a free oscillation amplitude of 3.88 nm (see equation (2)). The spring constant value was determined by finite element simulations using a model developed by our group resulting in $k \approx 34\,000$ [46, 47].

2.2. Functionalization of the biosensors and the test samples

For surface activation, several 1 × 1 cm pieces of glass coverslips and previously sharpened optical fibers (SiO_2) were immersed in a piranha solution (3:1 concentrated H_2SO_4 and 30% H_2O_2 solution) for 1 h, rinsed with MilliQ water and dried under nitrogen. After that, the substrates and fibers were placed in a mixture of $NH_4/H_2O_2/H_2O$ (1:1:5) for 30 min. Then, they were rinsed with Milli-Q water, blown dry with N_2 and stored in a dust-free environment. This process created SiOH functional hydroxyl groups on the surface for future modification.

For the functionalization of the fibers with biotin, aminosilanization was performed by immersing the activated fibers in a 2% in acetone solution of 3-aminopropyltriethoxysilane (APTES) and triethoxymethylsilane (TEMS) (Sigma-Aldrich, St. Louis, MO, USA) corresponding to APTES/TEMS (1:100) and leaving them overnight. Then, the fibers were rinsed with acetone three times, dried under N_2 and cured for 20 min at 90 °C. Next, the fibers were incubated in a solution of 20 μg ml^{-1} biotin *N*-hydroxysuccinimide ester in DMSO 1% (Sigma-Aldrich, St. Louis, MO, USA) in phosphate-buffered saline (PBS) (100 mM, pH 7.4) for 6 h. After that, the functionalized probes were rinsed twice in a PBS solution with EDTA 0.1% and triton x-100 1% for 15 min, twice in PBS for another 15 min and stored in PBS at 4 °C until used. The same procedure was followed to functionalize the AFM tips.

For the functionalization of the substrates with streptavidin (Sigma-Aldrich, St. Louis, MO, USA), the activated substrates were immersed overnight in a 2% solution in ethanol of triethoxysilylundecanal (TESUD) (ABCR, Germany) and (6-{2-[2-(2-methoxyethoxy)ethoxy]ethoxy}hexyl) trimethoxysilane (MTMS) (Sikemia, France) corresponding to TESUD/MTMS (1:100). Then, the samples were washed three times with ethanol, dried under N_2 and cured for 20 min at 90 °C. After that, substrates were incubated in a solution of 20 μg ml^{-1} streptavidin (Sigma-Aldrich, St. Louis, MO, USA) in PBS (100 mM, pH 7.4) with 5 mM of sodium cianoborohydride for 6 h. Finally, the functionalized probes were rinsed twice in a PBS solution with EDTA 0.1% and triton x-100 1% for 15 min, twice in PBS for another 15 min and stored in PBS at 4 °C until used.

To take a fluorescence image of the functionalized fibers with biotin, they were immersed for 30 min in a solution (20 μg ml^{-1}) of avidin labeled with Texas Red. After that, the functionalized probes were rinsed twice in a PBS solution with EDTA 0.1% and triton x-100 1% for 15 min. Figure 2 shows the optical images of the QTF probe functionalized with biotin and conjugated with Avidin—TR (DMIRB wide-field transmitted light and fluorescence microscope, Leica Microsystems, Germany).

2.3. Data acquisition and analysis

Experiments with standard AFM tips were performed using an AFM microscope (MFP-3D, Asylum Research, USA). The cantilevers used were made of silicon nitride with a nominal spring constant $K = 0.06$ N m^{-1} (PNP-DB type cant.B,

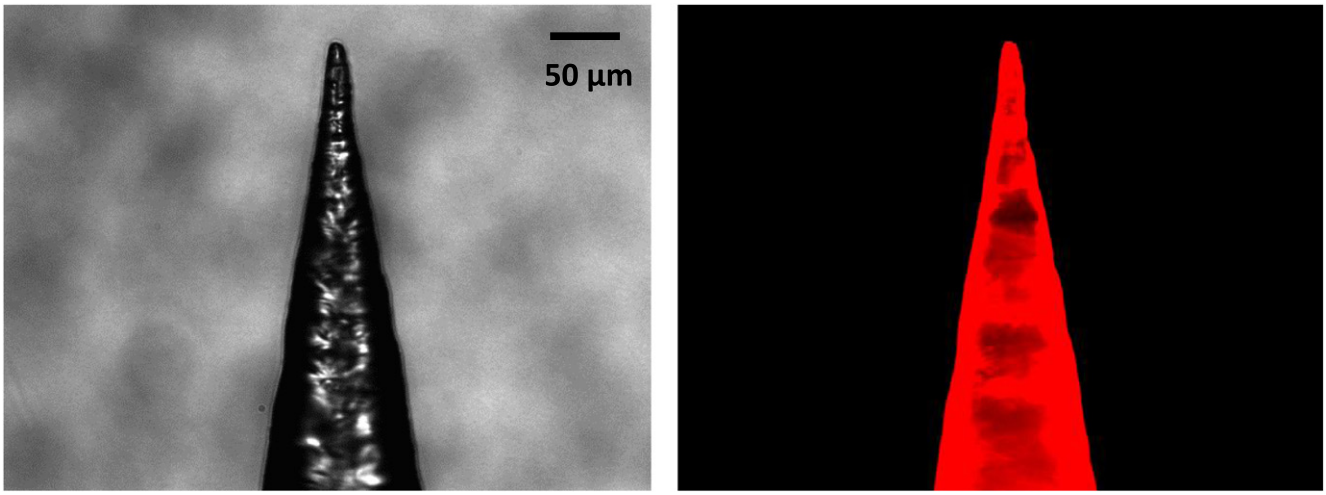

Figure 2. Tuning fork tip functionalized with biotin and conjugated with Avidin–Texas Red. Optical microscopy images with normal light (left) and fluorescence filters (right).

NanoAndMore GmbH, Germany). Independently, we calibrated the spring constant using thermal fluctuation analysis according to [48] and obtained a value of $K = 0.025\,\mathrm{N\,m^{-1}}$.

Force measurements were acquired by bringing the biotin-coated AFM tip or QTF probe into contact with the substrate functionalized with immobilized streptavidin in PBS at room temperature. The contact time between the probe and the surface was 1 s in all the experiments. The retraction speed was varied from 200 to $1000\,\mathrm{nm\,s^{-1}}$ whereas the approaching velocity was kept constant. The respective molecular loading rates were calculated by multiplying the experimental velocities by the measured molecular elasticities, which were determined from the force curve graphs [49]. All the data were consecutively analyzed according to the stochastic Bell–Evans model of a forced dissociation under an external load [50, 51].

The maximum indentation was controlled in both cases to minimize the contact area. Force–distance curves were acquired under identical conditions and individually analyzed with custom-made MATLAB-based analysis software (The MathWorks, Natick, MA) to calculate molecular adhesion forces and adhesion energies.

For AFM measurements, the adhesion energy was computed as the area under the force–distance retraction curve with the baseline taken at zero force. For QTF measurements, the first step is to translate the amplitude–distance curves into force–distance curves via equation (1) [52].

$$F = \left(1 - \frac{I}{I_0}\right)\frac{k_s A_0}{\sqrt{3}\,Q}, \tag{1}$$

$$A_0 = \sqrt{\frac{V I_0 Q}{k_s w_0}}. \tag{2}$$

The force curves are obtained according to equation (1) where I is the current measured through the QTF, I_0 is the current when the probe is far from the sample, k_s is the spring constant, Q is the quality factor and A_0 is the free oscillation amplitude. The mechanical vibration amplitude was calculated using the expression given by equation (2) [53], where V is the excitation voltage, I_0 is the current measured through the QTF, and w_0 is the free resonance frequency. Then, the area confined between approach and withdrawal lines is calculated to obtain the adhesion energy. In general, force and energy are correlated such that [54]:

$$E = -\int_{h_1}^{h_2} F\,\mathrm{d}h, \tag{3}$$

where E is the adhesion energy, F is the pull-off force, and h is the separation distance. To calculate the adhesion energy, the integral in equation (3) was evaluated using the Trapezoidal rule [54].

3. Results

Amplitude versus tip–sample distance curves were plotted by measuring the current, I_{rms}, through the QTF when the biotin-functionalized QTF probe was approaching and moving away from the immobilized streptavidin on the sample surface at different retraction speeds. The QTF was driven at the resonance frequency; I_{rms} was constant when the probe was far from the sample surface and diminished as the QTF approached the sample. Figures 3(b) and (c), show two representative graphs of an amplitude–displacement curve for the biotin–streptavidin system for two speeds of retraction: $300\,\mathrm{nm\,s^{-1}}$ and $440\,\mathrm{nm\,s^{-1}}$, respectively. We checked the specificity of the interaction by adding free biotin which cancels the adhesion forces. The approach and withdrawal curves are almost identical without showing any distinct non-linear jumps. Interestingly, however, we observed hysteresis between the approach and the retraction curves, indicating that there is an interaction between the biotin–streptavidin complexes [55]. The area confined between the approach and withdrawal curves is related to bond energy and it increases with retraction speed. Control curves over a non-

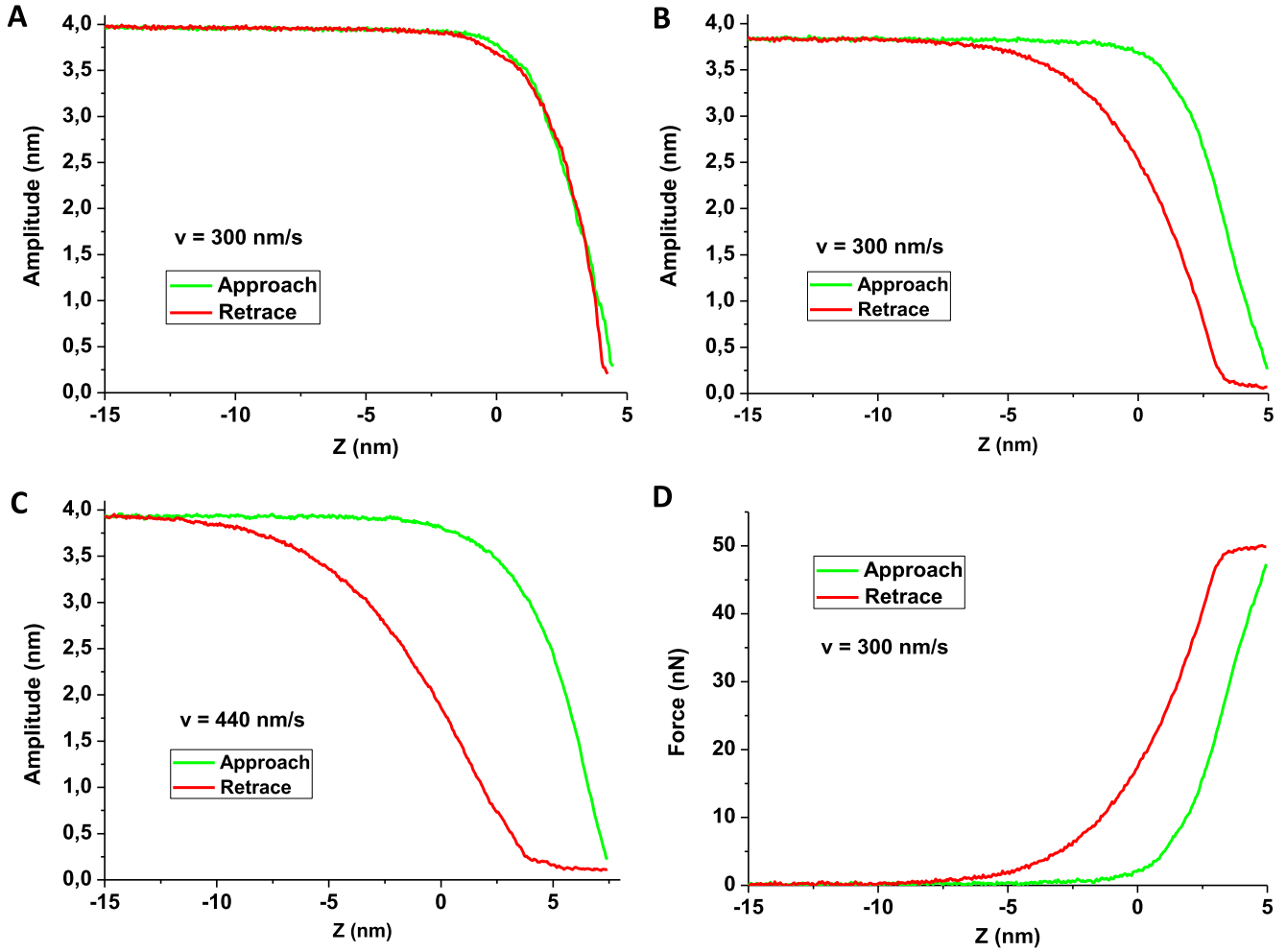

Figure 3. (A) Amplitude versus tip–sample distance control curve over a non-functionalized bare glass surface. Same control curves are obtained when free biotin is added into the solution. (B), (C) Representative amplitude–distance curves of the interaction between a biotin-functionalized QTF probe over streptavidin immobilized on the sample surface at retraction speeds of 300 nm s^{-1} and 400 nm s^{-1} respectively. (D) Amplitude–distance curve at 300 nm s^{-1} (showed in graph B) translated into force–distance curve by using equations (1) and (2).

functionalized bare glass surface were performed to confirm that the measured hysteresis was due to the specific interaction between the biotin–streptavidin systems and no hysteresis is observed in this case (see figure 3). Similar amplitude–distance curves were obtained when free biotin (0.1 mg ml^{-1}) was added to the solution showing that interaction was inhibited and therefore, the probability of bond formation was drastically reduced (∼5% of trials).

The amplitude–distance curves which presented hysteresis (∼65% of trials) are translated to force curves for each retraction speed using equation (1) as illustrated in figure 3(D). The area confined between the approach and retraction curves is calculated to obtain the energy. Histograms of adhesion energies from some 100 interactions for each speed are presented in figure 4 where a Gaussian function is fitted to each one to extract the mean adhesion energy for each retraction velocity.

The same measurements were performed with a standard AFM tip and several force–distance curves were acquired under the same conditions. Figure 5 shows a representative

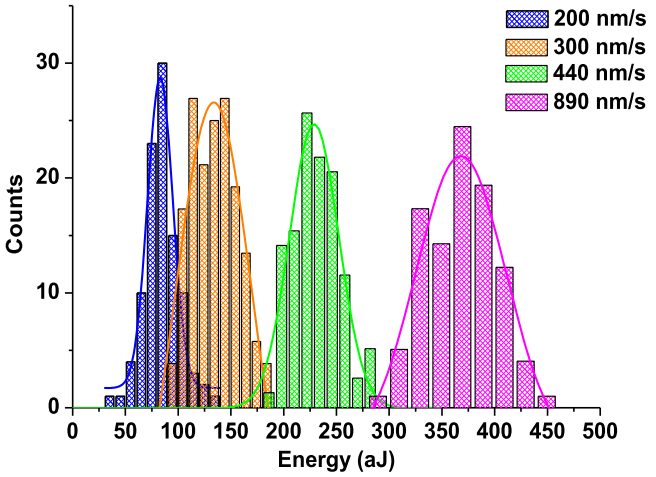

Figure 4. (A) Histograms of the adhesion energy between a biotin QTF probe and streptavidin surface at retraction speeds of (I) 200 nm s^{-1} (II) 300 nm s^{-1} (III) 440 nm s^{-1} and (IV) 890 nm s^{-1}. All the histograms were fitted to a Gaussian function. The centers of the energy distribution were (I) 83 ± 12 aJ (II) 135 ± 36 aJ (III) 228 ± 23 aJ and (IV) 369 ± 43 aJ.

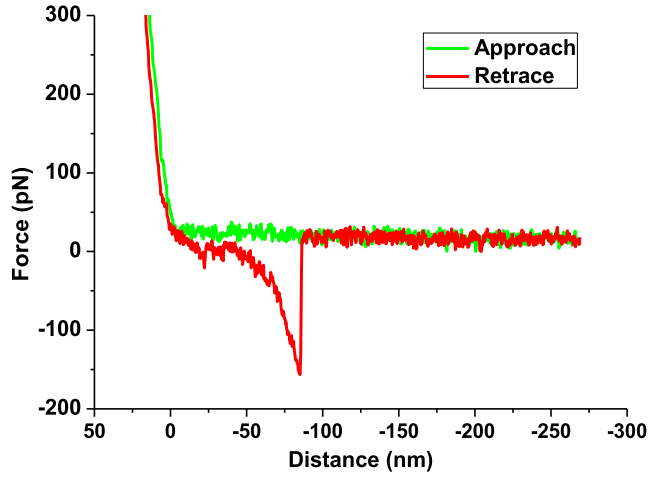

AFM		
Speed (nm/s)	*F (pN)*	*Energy (aJ)*
300	137 ± 49	1.2 ± 0.3
500	193 ± 67	2.5 ± 0.7
700	212 ± 64	3.2 ± 1.1
1000	218 ± 49	4.0 ± 1.5

Figure 5. Representative force–distance curve of the interaction between biotin-functionalized AFM tip over streptavidin immobilized on the sample surface at a retraction speed of 500 nm s^{-1}. Table: mean rupture forces F and adhesion energies for each pulling velocity.

force curve of the interaction of the biotin–streptavidin system at a retraction speed of 500 nm s^{-1}, corresponding to a loading rate of 5200 pN s^{-1}. The adhesion energy E was determined by integrating the area of each single-molecule event in the force–distance curves. We found single-molecule adhesion energies of $E = 1.2$–4 aJ at a binding probability of >60%. These energies are about two orders of magnitude smaller than those observed by QTF force spectroscopy and reflect the fact that fewer molecules are probed in AFM experiments. In this case, it was possible to obtain the unbinding forces F of each single event. Mean rupture forces F and adhesion energies for each pulling velocity are summarized in table of figure 5.

4. Discussion

As a novel technology, QTF-based nanosensors for nano-characterization are constantly being improved through different advances in instrumentation and the emergence of new applications. In spite of the great potential of the technique to detect specific interactions between ligand and receptor, the capacity to measure discrete interactions is compromised. Because the binding force of an individual molecular pair is not known, the number of interacting molecules cannot be determined exactly. The total number of streptavidin–biotin bonds formed in an experiment depends on receptor density, contact duration and the area of contact. Moreover, it is difficult to quantify the unbinding force because there is no complete mechanical model of the QTF sensor to provide the magnitude of the measured forces when working in shear mode. However, following the same procedure as in [56], it is possible to arrive to an approximation of the number of bonds in a given measurement. From the adhesion energy value from measurements of the QTF at a speed of 300 nm s^{-1}, the binding force can be approximated as the adhesion energy divided by the binding length, about 0.8 nm [57], resulting in 175 nN. We can also consider the estimated binding force per streptavidin–biotin pair measured with the standard AFM tip,

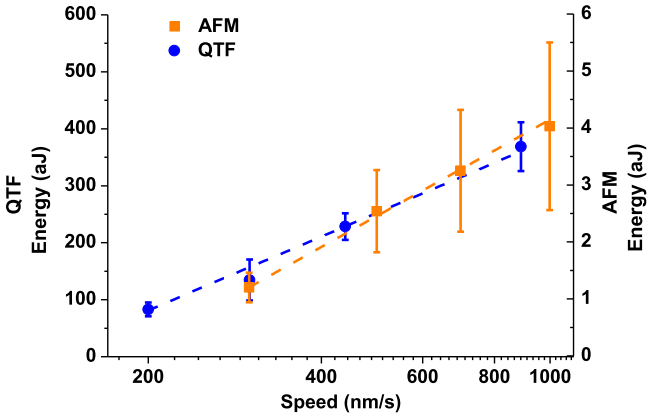

Figure 6. Representation of the adhesion energy of the biotin–streptavidin complex versus retraction speed with a logarithmic scale measured with conventional AFM tips and QTF probes. Fitted linear regression functions: $y = 4.7 \log x - 12.7$ and $y = 430 \log x - 909$ for AFM and QTF results respectively.

which is 137 pN at the same pulling speed of 300 nm s^{-1}. Under this assumption, the adhesion between the biotin tip and the streptavidin surface in our experiments with QTF corresponds to a contribution from about 1275 molecular pairs. Furthermore, if we assume a dense coverage of the surface with streptavidin (30 nm^2 per molecule of streptavidin) then the interaction area is equivalent to half the area of a sphere with a radius of 78 nm. This value is close to the probe radius obtained from the etched fibers, which is around 100 nm. This would mean that in our experiment, 80% of the entire curvature of the tip contributes to the adhesion. Taking account of this assumption, we can estimate that the difference between the adhesion energies obtained with the QTF probe and the AFM tip is basically due to the contact area, since the tip radius in the QTF probe is approximately 10 times larger than the AFM tip radius (nominal radius considered as ~10 nm). This means a relation of 100 times in terms of contact area. Figure 6 shows the results of adhesion energies measured with both the QTF and AFM sensors,

which can be compared. Interestingly, although the magnitude of the measured energies are different by 2 orders of magnitude, the tendency of both results is equivalent, showing great proportionality between them in a factor of 100. We think that this proportionality constant could be related to the difference in the contact area between the sensors due to the different tip radii.

Measuring the unbinding forces at different pulling speeds it is possible to extract the dissociation kinetics of the studied molecular bond. To achieve single-molecule measurements with the tuning fork probes, it is necessary to improve glass fiber apexes, in order to get an effective radius of tenths of nanometers (comparable to standard AFM probes). With this goal, authors have been recently developed a method based on attaching a standard AFM tip to the end of a fiber probe which has previously been sharpened [61]. Future experiments with these probes will allow the measurement of single-molecule interactions, which will be the key to determine the ultimate resolution of the system and its capabilities to differentiate between different molecular interactions.

5. Conclusions

The main purpose of this work is to prove that QTF biosensors are capable of quantitatively measuring the interaction between proteins. In this way, we have been able to quantify the results and compare them with those obtained with a conventional AFM microscope. We have presented a new procedure based on AFM DFS applied to QTF-based nanosensors for molecular interaction studies. By using this procedure, the adhesion energy of the biotin–streptavidin complex has been analyzed, obtaining results comparable to those measured with a conventional AFM tip. Nevertheless, tapered glass fiber apexes should be improved for the purpose of achieving single-molecule measurements. Our results show good agreement between QTF and AFM experiments, so they open the door to the use of QTFs as biosensors in biomolecular measurements in liquid conditions, in compact solutions where a laser-free detection scheme is needed.

Acknowledgments

The authors thank F Rico from INSERM Marseille for fruitful discussions. This work was supported by the Spanish Ministerio de Ciencia e Innovación through Projects TEC2009-10114 and TEC2011-29140-C03-02 and grant BES-2010-031186.

Appendix. Consistency of the results by the calculation of the dissociation rate constant

In standard AFM measurements, it is possible to obtain the common dynamic spectrum from unbinding forces and loading rates to extract the dissociation kinetics of the streptavidin–biotin complex. The rupture force of these linkages was determined from the magnitude of the measured force peaks and was measured at different force loading rates. Variation in the loading rate L_r of the AFM measurements was achieved with different cantilever retraction rates v. L_r is the product of the system spring constant, k_s and v: $L_r = k_s\, x\, v$. The system spring constant depends on the elastic properties of both the cantilever and the substrate to which the streptavidin is attached. The measured system spring constants were in the range of 8.6–12 mN m^{-1} and were obtained from the slope of the force versus displacement relationship of each single event. Consequently, the loading rate of the force measurements was varied from 2600 to 12 000 pN s^{-1} to cover only one energy barrier. According to Bell–Evans theory [50, 58], the dependence of the unbinding force F on the force loading rate L_r follows the relationship of equation (4). Here, k_B is Boltzmann's constant, k_0 is the dissociation rate constant in the absence of applied force and x_β is the reaction length.

$$F = \frac{k_B T}{x_\beta} \ln\left(\frac{L_r x_\beta}{k_0 k_B T}\right). \tag{4}$$

Plotting the rupture force F versus $\ln(L_r)$, it is possible to estimate the reaction length, x_β, for a given regime of applied external forces from the slope of the line fitted to experimental data in the force spectrum plot. The dissociation rate constant, k_0, can be deduced by linearly extrapolating the data to zero external force ($F = 0$). The results were $k_0 = 3.74$ s^{-1} and $x_\beta = 0.08$ nm which agree with the values founded in the literature. For instance, a value of $k_0 = 2.98 \pm 2.61$ s^{-1} and $x_\beta = 0.024$ nm for L_r between 1700 and 9600 pN s^{-1} and $k_0 = 2.09$ s^{-1} and $x_\beta = 0.05$ nm for L_r of 1000–5000 pN s^{-1} were reported respectively in [59] and [60].

References

[1] Dufrêne Y F 2009 Atomic force microscopy: a powerful molecular toolkit in nanoproteomics *Proteomics* **9** 5400–5
[2] Dufrêne Y F, Evans E, Engel A, Helenius J, Gaub H and Müller D 2011 Five challenges to bringing single-molecule force spectroscopy into living cells *Nat. Methods* **8** 123–7
[3] Ivanov A A, Khuri F R and Fu H 2013 Targeting protein–protein interactions as an anticancer strategy *Trends Pharmacol. Sci.* **34** 393–400
[4] Wang Q and Moerner W E 2014 Single-molecule motions enable direct visualization of biomolecular interactions in solution *Nat. Methods* **11** 555–8
[5] Yildirim M A, Goh K I, Cusick M E, Barabasi A L and Vidal M 2007 Drug-target network *Nat. Biotechnol.* **25** 1119–26
[6] Bakheet T M and Andrew J D 2009 Properties and identification of human protein drug targets *Bioinformatics* **25** 451–7
[7] Giacomini K M 2010 Membrane transporters in drug development *Nat. Rev. Drug Discovery* **9** 215–36
[8] Ritort F 2006 Single-molecule experiments in biological physics: methods and applications *J. Phys.: Condens. Matter* **18** R531–83

[9] Neuman K C and Nagy A 2008 Single-molecule force spectroscopy: optical tweezers, magnetic tweezers and atomic force microscopy *Nat. Methods* **5** 491–505

[10] Bippes C A and Muller D J 2011 High-resolution atomic force microscopy and spectroscopy of native membrane proteins *Rep. Prog. Phys.* **74** 086601

[11] Lin S, Wang Y, Huang L, Lin C, Hsu S and Lee C 2007 Dynamic response of glucagon/anti-glucagon pairs to pulling velocity and pH studied by atomic force microscopy *Biosens. Bioelectron.* **22** 1013–9

[12] Andre G, Kulakauskas S, Chapot-Chartier M P, Navet B, Deghorain M, Bernard E, Hols P and Dufrêne Y F 2010 Imaging the nanoscale organization of peptidoglycan in living *Lactococcus lactis* cells *Nat. Commun.* **1** 27

[13] Li M, Xiao X, Liu L, Xia N, Wanga Y, Donga Z and Zhang W 2013 Atomic force microscopy study of the antigen antibody binding force on patient cancer cells based on ROR1 fluorescence recognition *J. Mol. Recognit.* **26** 432–8

[14] Florin E L, Moy V T and Gaub H E 1994 Adhesion forces between individual ligand–receptor pairs *Science* **264** 415–7

[15] Lee G U, Kidwell D A and Colton R J 1994 Sensing discrete streptavidin biotin interactions with atomic-force microscopy *Langmuir* **10** 354–7

[16] Moy V T, Florin E L and Gaub H E 1994 Intermolecular forces and energies between ligands and receptors *Science* **266** 257–9

[17] Lee C, Wang Y, Huang L and Lin S 2007 Atomic force microscopy: determination of unbinding force, off rate and energy barrier for protein–ligand interaction *Micron* **38** 446–61

[18] Fuhrmann A and Ros R 2010 Single-molecule force spectroscopy: a method for quantitative analysis of ligand–receptor interactions *Nanomedicine* **5** 657–66

[19] Dammer U, Hegner M, Anselmetti D, Wagner P, Dreier M, Huber W and Güntherodt H J 1996 Specific antigen/antibody interactions measured by force microscopy *Biophys. J.* **70** 2437–41

[20] Fuhrmann A, Schoning J, Anselmetti D, Staiger D and Ros R 2009 Quantitative analysis of single-molecule RNA–protein interaction *Biophys. J.* **96** 5030–9

[21] Nettikadan S R, Johnson J C, Vengasandra S G, Muys J and Henderson E 2004 ViriChip: a solid phase assay for detection and identification of viruses by atomic force microscopy *Nanotechnology* **15** 383–9

[22] Schoenwald K, Peng Z C, Noga D, Qiu S R and Sulchek T 2010 Integration of atomic force microscopy and a microfluidic liquid cell for aqueous imaging and force spectroscopy *Rev. Sci. Instrum.* **81** 053704

[23] Quist A, Chand A, Ramachandran S, Cohena D and Lal R 2006 Piezoresistive cantilever based nanoflow and viscosity sensor for microchannels *Lab. Chip* **6** 1450–4

[24] Moldovan N, Kim K and Espinosa H D 2006 Design and fabrication of a novel microfluidic nanoprobe *J. Microelectromech. Syst.* **15** 1

[25] Yin T, Zhao Y, Horak J, Bakirci H, Liao H H, Tsai H H, Juang Y Z and Urban G 2013 A micro-cantilever sensor chip based on contact angle analysis for a label-free troponin I immunoassay *Lab. Chip* **13** 834

[26] Giessibl F J 2003 Advances in atomic force microscopy *Rev. Mod. Phys.* **75** 949–83

[27] Polesel-Maris J, Lubin C, Thoyer F and Cousty J 2011 Combined dynamic scanning tunneling microscopy and frequency modulation atomic force microscopy investigations on polythiophene chains on graphite with a tuning fork sensor *J. Appl. Phys.* **109** 074320

[28] Lange M, van Vörden D and Möller R 2012 A measurement of the hysteresis loop in force–spectroscopy curves using a tuning-fork atomic force microscope *Beilstein J. Nanotechnology* **3** 207–12

[29] Welker J and Giessibl F J 2012 Revealing the angular symmetry of chemical bonds by atomic force microscopy *Science* **336** 444–9

[30] Rensen W H J, van Hulst N F and Kämmer S B 2000 Imaging soft samples in liquid with tuning fork based shear force microscopy *Appl. Phys. Lett.* **77** 1557

[31] Otero J, González L and Puig-Vidal M 2012 Nanocharacterization of soft biological samples in shear mode with quartz tuning fork probes *Sensors* **12** 4803–19

[32] Makky A, Viel P, Chen S W, Berthelot T, Pellequer J and Polesel-Maris J 2013 Piezoelectric tuning fork probe for atomic force microscopy imaging and specific recognition force spectroscopy of an enzyme and its ligand *J. Mol. Recognit.* **26** 521–31

[33] Wutscher E and Giessibl F J 2011 Atomic force microscopy at ambient and liquid conditions with stiff sensors and small amplitudes *Rev. Sci. Instrum.* **82** 093703

[34] Ruiter A G T, Veerman J A, van der Werf K O and van Hulst N F 1997 Dynamic behavior of tuning fork shear-force feedback *Appl. Phys. Lett.* **71** 149–57

[35] Matsko N B 2011 Self-sensing and actuating probes for tapping mode AFM measurements of soft polymers at a wide range of temperatures *J. Mod. Phys.* **2** 72–8

[36] Karrai K and Tiemann I 2000 Interfacial shear force microscopy *Phys. Rev.* B **62** 13174

[37] Otero J, Baños R, Gonzalez L, Torrents E, Juarez A and Puig-Vidal M 2013 Quartz tuning fork studies on the surface properties of Pseudomonas aeruginosa during early stages of biofilm formation *Colloids Surf.* B **102** 117–23

[38] González L, Otero J, Agusil J P, Samitier J, Adan J, Mitjans F and Puig-Vidal M 2014 Micropattern of antibodies imaged by shear force microscopy: comparison between classical and jumping modes *Ultramicroscopy* **136** 176–84

[39] Makky A, Berthelot T, Feraudet-Tarisse C, Volland H, Viel P and Polesel-Maris J 2012 Substructures high resolution imaging of individual IgG and IgM antibodies with piezoelectric tuning fork atomic force microscopy *Sensors Actuators* B **162** 269–77

[40] Hofer M *et al* 2010 Molecular recognition imaging using tuning fork-based transverse dynamic force microscopy *Ultramicroscopy* **110** 605

[41] Polesel-Maris J, Legrand J, Berthelot T, Garcia A, Viel P, Makky A and Palacin S 2012 Force spectroscopy by dynamic atomic force microscopy on bovine serum albumin proteins changing the tip hydrophobicity, with piezoelectric tuning fork self-sensing scanning probe *Sensors Actuators* B **161** 775–83

[42] Harder A, Walhorn V, Dierks T, Fernàndez-Busquets X and Anselmetti D 2010 Single-molecule force spectroscopy of cartilage aggrecan self-adhesion *Biophys. J.* **99** 3498–504

[43] Gordesli F P and Abu-Lail N I 2012 The role of growth temperature in the adhesion and mechanics of pathogenic *L. monocytogenes*: an AFM study *Langmuir* **28** 1360–73

[44] Mononobe S 2005 *Near-Field Optical Fiber Probes and the Imaging Applications: Progress in Nano-Electro-Optics III* (Berlin: Springer)

[45] González L, Otero J, Cabezas G and Puig-Vidal M 2012 Electronic driver with amplitude and quality factor control to adjust the response of quartz tuning fork sensors in atomic force microscopy applications *Sensors Actuators* A **184** 112–8

[46] Oria R, Otero J, González L, Botaya L, Carmona M and Puig-Vidal M 2013 Finite element analysis of electrically excited quartz tuning fork devices *Sensors* **13** 7156–69

[47] Gonzalez L, Oria R, Botaya L, Puig-Vidal M and Otero J 2015 Determination of the static spring constant of electrically-driven quartz tuning forks with two freely oscillating prongs *Nanotechnology* **26** 055501

[48] Hutter J L and Bechhoefer J 1993 Calibration of atomic-force microscope tips *Rev. Sci. Instrum.* **64** 1868
[49] Fuhrmann A, Anselmetti D and Reimann P 2008 Refined procedure of evaluating experimental single-molecule force spectroscopy data *Phys. Rev.* E **68** 045103
[50] Evans E and Ritchie K 1997 Dynamic strength of molecular adhesion bonds *Biophys. J.* **72** 1541–55
[51] Merkel R, Nassoy P and Evans E 1999 Energy landscapes of receptor–ligand bonds explored with dynamic force spectroscopy *Nature* **397** 50–3
[52] Karraï K and Grober R D 1995 Piezo-electric tuning fork tip-sample distance control for near field optical microscopes *Ultramicroscopy* **61** 197–205
[53] Liu J, Callegari A, Stark M and Chergui M 2008 A simple and accurate method for calibrating the oscillation amplitude of tuning-fork based AFM sensors *Ultramicroscopy* **109** 81–4
[54] Cox M G 2007 The area under a curve specified by measured values *Metrologia* **44** 365–78
[55] Lange M, van Vörden D and Möller R 2012 A measurement of the hysteresis loop in force–spectroscopy curves using a tuning-fork atomic force microscope *Beilstein J. Nanotechnology* **3** 207–12
[56] Moy V T, Florin E L and Gaub H E 1994 Adhesive forces between ligand and receptor measured by AFM *Colloids Surf.* A **93** 343–8
[57] Livnah 0, Bayer E A, Wilchck M and Sussman J L 1993 Three-dimensional structures of the avidin and the avidin-biotin complex *Proc. Natl Acad. Sci. USA* **90** 5076
[58] Bell G I 1978 Models for specific adhesion of cells to cells *Science* **200** 618–27
[59] Piramowicz M O, Czuba P, Targosz M, Burda K and Szymoński M 2006 Dynamic force measurements of avidin–biotin and streptavidin–biotin interactions using AFM *Acta Biochim. Pol.* **53** 93–100
[60] Yuan C, Chen A, Kolb P and Moy V T 2000 Energy landscape of streptavidin–biotin complexes measured by atomic force microscopy *Biochemistry* **39** 10219–23
[61] Gonzalez L, Martínez-Martín D, Otero J, de Pablo P J, Puig-Vidal M and Gómez-Herrero J 2015 Improving the lateral resolution of quartz tuning fork-based sensors in liquid by integrating commercial AFM tips into the fiber end *Sensors* **15** 1601–10